

On-site correlation in valence and core states of ferromagnetic nickel

F. Manghi and V. Bellini

*Istituto Nazionale per la Fisica della Materia and Dipartimento di Fisica, Università di Modena, Via Campi 213/a,
I-41100 Modena, Italy*

C. Arcangeli

Max-Planck-Institut für Festkörperforschung, Heisenbergstrasse 1, D-70569 Stuttgart, Germany

(Received 19 February 1997)

We present a method which allows us to include narrow-band correlation effects in the description of both valence and core states and we apply it to the prototypical case of nickel. The results of an *ab initio* band calculation are used as input mean-field eigenstates for the calculation of self-energy corrections and spectral functions according to a three-body scattering solution of a multiorbital Hubbard Hamiltonian. The calculated quasiparticle spectra show a remarkable agreement with photoemission data in terms of bandwidth, exchange splitting, satellite energy position of valence states, and spin polarization of both the main line and the satellite of the $3p$ core level. [S0163-1829(97)01435-5]

I. INTRODUCTION

It is well established that the description of electronic states in narrow-band materials requires improvements over the single-particle approximation with a proper inclusion of on-site Coulomb interaction between localized electrons.¹ In these systems the itinerant character of valence electrons which is clearly shown by the energy k dispersion observed in photoemission spectroscopy coexists with strong local electronic correlation responsible for other observed features such as satellite structures and band-narrowing effects. The interplay of localization and itinerancy has also been indicated as a possible explanation of the observed spin polarization of core-level spectra through exchange coupling between localized (core) and itinerant (valence) states.^{2,3}

In this paper we present a theoretical description of the valence and core electron states of nickel according to a method recently developed which has been designed to treat highly correlated and highly hybridized systems⁴ including both the itinerant character of band electrons and the strong localized electron-electron repulsion. This method allows us to include narrow-band correlation effects in a first-principles band calculation; the single-particle band states are determined according to the density functional theory in the local density approximation (LDA) and the correlation effects are described as a three-body scattering (3BS) solution of a multiorbital Hubbard Hamiltonian. This approach has been previously applied to the description of valence and conduction states of both model systems^{5,6} and realistic materials.^{4,7,8} We present here an extension of the method in order to treat both valence and core states on the same footing; this extension is possible in this scheme since it relies on a multiorbital Hubbard Hamiltonian where core and valence states can coexist and on the 3BS method which can be applied for any value of effective on-site electron-electron repulsion.

As far as the valence states are concerned various methods have been proposed to augment conventional band theory for the description of the electronic states of nickel;

some of them are based on perturbative expansion either in the e - e interaction (GW approach,⁹ second-order solution of the Hubbard Hamiltonian¹⁰⁻¹²) or in the fluctuations of the electron occupation around LDA mean-field solution;¹³ others apply a t -matrix scheme where the effect of electron correlation on one-electron removal energies from a partially filled band is described as a hole-hole interaction.^{14,15} This method is strictly valid only in the limit of an almost filled band (dilute limit) and its application to the case of nickel has been questioned.¹⁰ In order to implement this approach it is necessary to include also electron-electron scattering channels and to solve a three-body scattering problem involving two holes and one electron. This is the spirit of the 3BS theory we apply here and which has been originally formulated by Igarashi.⁵ This approach has recently been applied to the description of valence states of nickel¹⁶ choosing, however, an approximate form of self-energy in terms of the antisymmetrized vertex function; in this way the self-energy turns out to be real, giving rise to peaks in the spectral density of unphysical zero width. Here we will instead adopt a version of the theory which avoids this shortcoming and which is based on the explicit solution of the three-body scattering equations.^{4,6,7}

The interpretation of core-level spectroscopies has up to now largely been based on atomic models which interpret the structures observed in the one-electron removal spectra in terms of multiplet states formed by coupling the core hole to the unfilled valence shell.¹⁷ This scheme has in particular been applied to the photoemission spectra from the core states of transition metals¹⁸ attributing the observed characteristic line splitting to intra-atomic exchange interaction between core and valence electrons of an isolated atom. Such an approach has been seriously questioned since the observed splittings and the energy scale of the interaction are of the same order of magnitude as the valence band width;² a picture which takes into account the itinerant character of valence electrons seems therefore necessary. With the advent of spin-polarized spectroscopies such as spin-resolved x-ray photoemission^{3,19} and magnetic circular dichroism²⁰ the spin

dependence of both the main line and the satellites of Ni core-level spectra has been widely investigated.^{19,21–23} We will show that the 3BS solution of a multiband Hubbard Hamiltonian, where full details of the valence band structure are included, can account for these spectroscopical features and interpret them in terms of on-site interaction between localized (core) and itinerant (valence) states.

The paper is organized as follows: we present in Sec. II the multiorbital Hubbard Hamiltonian and its relationship to the band Hamiltonian we want to implement; Sec. III describes the main characteristics of the method which we use to get an approximate solution of the Hubbard Hamiltonian in terms of self-energy corrections to band eigenstates and of spectral densities; Secs. IV and V specialize to the case of valence and core states, respectively; the results and the comparison with experiments are presented in Sec. VI.

II. MULTIBAND HUBBARD HAMILTONIAN

Band structure eigenvalues are in many cases good zero-order approximations to the excitation spectrum of a solid and it seems reasonable to use them as a starting point for the inclusion of correlation effects according to the Hubbard model; the implicit assumption is that among all the many-body terms responsible for electron correlation, the Coulomb repulsion between electrons on the same site is the one which needs to be treated explicitly. To do this it is necessary to define precisely the relationship between band and Hubbard Hamiltonian. Let us consider first a localized basis set $\phi_{i\alpha\sigma}(\mathbf{r},s)$ with i labeling the localization site, α the orbital character, and s and σ the spin coordinate and eigenvalue, respectively. The full many-body Hamiltonian in second quantization is

$$\hat{H} = \sum_{i\alpha\sigma} \epsilon_{i\alpha\sigma}^0 \hat{n}_{i\alpha\sigma} + \sum_{\alpha\beta\sigma} \sum_{ij} t_{i\alpha,j\beta} \hat{c}_{i\alpha\sigma}^\dagger \hat{c}_{j\beta\sigma} + \frac{1}{2} \sum_{i\alpha,j\beta,l\gamma\sigma',m\delta\sigma} \sum_{\sigma\sigma'} V_{i\alpha\sigma,j\beta\sigma',l\gamma\sigma',m\delta\sigma} \hat{c}_{i\alpha\sigma}^\dagger \hat{c}_{j\beta\sigma'}^\dagger \hat{c}_{l\gamma\sigma'} \hat{c}_{m\delta\sigma},$$

with $\hat{n}_{i\alpha\sigma} = \hat{c}_{i\alpha\sigma}^\dagger \hat{c}_{i\alpha\sigma}$ and $\hat{c}_{i\alpha\sigma}, \hat{c}_{i\alpha\sigma}^\dagger$ destruction and creation operators.

Here $\epsilon_{i\alpha\sigma}^0$ and $t_{i\alpha,j\beta}$ are the intra-atomic and interatomic matrix elements of the one-particle Hamiltonian (kinetic energy plus ionic potential), while $V_{i\alpha\sigma,j\beta\sigma',l\gamma\sigma',m\delta\sigma}$ are multicenter integrals involving the electron-electron interaction,

$$V_{i\alpha\sigma,j\beta\sigma',l\gamma\sigma',m\delta\sigma} = \sum_{s's'} \int \phi_{i\alpha\sigma}^*(\mathbf{r},s) \phi_{j\beta\sigma'}^*(\mathbf{r}',s') \times \frac{e^2}{|\mathbf{r}-\mathbf{r}'|} \phi_{l\gamma\sigma'}(\mathbf{r}',s') \phi_{m\delta\sigma}(\mathbf{r},s) d\mathbf{r}d\mathbf{r}'.$$

In this last expression the dominant contribution comes from the one-center integrals with $i=j=l=m$ which are the usual on-site Coulomb term

$$U_{\alpha\beta}^i = V_{i\alpha\sigma,i\beta\sigma,i\alpha\sigma} = V_{i\alpha\sigma,i\beta-\sigma,i\beta-\sigma,i\alpha\sigma}$$

and exchange term

$$J_{\alpha\beta}^i = V_{i\alpha\sigma,i\beta\sigma,i\alpha\sigma,i\beta\sigma}.$$

The full many-body Hamiltonian can then be written as

$$\hat{H} = \sum_{i\alpha\sigma} \epsilon_{i\alpha\sigma} \hat{n}_{i\alpha\sigma} + \sum_{\alpha\beta\sigma} \sum_{ij} t_{i\alpha,j\beta} \hat{c}_{i\alpha\sigma}^\dagger \hat{c}_{j\beta\sigma} + \frac{1}{2} \sum_{\alpha\beta} \left[\sum_i (U_{\alpha\beta}^i - J_{\alpha\beta}^i) \sum_{\sigma} \hat{n}_{i\alpha\sigma} \hat{n}_{i\beta-\sigma} \right] + \dots \text{(multicenter terms)}. \quad (2.1)$$

Different approximations of the exact Hamiltonian (2.1) can be obtained using a mean-field approach which amounts to neglecting fluctuations in the electron occupation,

$$\begin{aligned} \hat{n}_{i\alpha\sigma} \hat{n}_{i\beta\sigma'} &= \hat{n}_{i\alpha\sigma} \langle \hat{n}_{i\beta\sigma'} \rangle + \hat{n}_{i\beta\sigma'} \langle \hat{n}_{i\alpha\sigma} \rangle - \langle \hat{n}_{i\alpha\sigma} \rangle \langle \hat{n}_{i\beta\sigma'} \rangle \\ &\quad + (\hat{n}_{i\alpha\sigma} - \langle \hat{n}_{i\alpha\sigma} \rangle) (\hat{n}_{i\beta\sigma'} - \langle \hat{n}_{i\beta\sigma'} \rangle) \\ &\simeq \hat{n}_{i\alpha\sigma} \langle \hat{n}_{i\beta\sigma'} \rangle + \hat{n}_{i\beta\sigma'} \langle \hat{n}_{i\alpha\sigma} \rangle - \langle \hat{n}_{i\alpha\sigma} \rangle \langle \hat{n}_{i\beta\sigma'} \rangle, \end{aligned}$$

where $\langle \rangle$ means a ground state average. The mean-field approximation can be applied to all the many-body terms of Eq. (2.1) transforming it into a single-particle Hamiltonian

$$\hat{H}^{\text{MF}} = \sum_{i\alpha\sigma} \epsilon_{i\alpha\sigma}^{\text{MF}} \hat{n}_{i\alpha\sigma} + \sum_{\alpha\beta\sigma} \sum_{ij} t_{i\alpha,j\beta} \hat{c}_{i\alpha\sigma}^\dagger \hat{c}_{j\beta\sigma}. \quad (2.2)$$

Any band structure calculation, where the interacting system is described as an effective single-particle problem, corresponds to the self-consistent solution of \hat{H}^{MF} . Another possibility is to apply the mean-field approximation selectively to the multicenter integrals, keeping the full many-body character in the one-center terms; in this way one gets a generalized Hubbard model

$$\begin{aligned} \hat{H}^H &= \sum_{i\alpha\sigma} \epsilon_{i\alpha\sigma}^H \hat{n}_{i\alpha\sigma} + \sum_{\alpha\beta\sigma} \sum_{ij} t_{i\alpha,j\beta} \hat{c}_{i\alpha\sigma}^\dagger \hat{c}_{j\beta\sigma} \\ &\quad + \frac{1}{2} \sum_{\alpha\beta} \left[\sum_i (U_{\alpha\beta}^i - J_{\alpha\beta}^i) \sum_{\sigma} \hat{n}_{i\alpha\sigma} \hat{n}_{i\beta\sigma} \right. \\ &\quad \left. + \sum_i U_{\alpha\beta}^i \sum_{\sigma} \hat{n}_{i\alpha\sigma} \hat{n}_{i\beta-\sigma} \right]. \end{aligned} \quad (2.3)$$

Since H^{MF} and H^H differ for the treatment of the on-site correlation — included in H^{MF} as a mean-field and treated as a many-body term in H^H — it is easy to show that

$$\epsilon_{i\alpha\sigma}^{\text{MF}} = \epsilon_{i\alpha\sigma}^H + \sum_{\beta} [(U_{\alpha\beta}^i - J_{\alpha\beta}^i) \langle \hat{n}_{i\beta\sigma} \rangle + U_{\alpha\beta}^i \langle \hat{n}_{i\beta-\sigma} \rangle]. \quad (2.4)$$

Due to the translational periodicity we can introduce an extended Bloch basis set

$$\psi_{\mathbf{k}\sigma}^n(\mathbf{r},s) = \frac{1}{\sqrt{N}} \sum_{i\alpha} C_{\alpha\sigma}^n(\mathbf{k}) e^{i\mathbf{k}\cdot\mathbf{R}_i} \phi_{i\alpha\sigma}(\mathbf{r},s) \quad (2.5)$$

and the corresponding relations for creation/destruction operators of electrons with wave vector \mathbf{k} , spin σ , and band index n ,

$$\hat{a}_{\mathbf{k}\sigma}^n = \frac{1}{\sqrt{N}} \sum_{i\alpha} C_{\alpha\sigma}^n(\mathbf{k}) e^{i\mathbf{k}\cdot\mathbf{R}_i} \hat{c}_{i\alpha\sigma},$$

$$\hat{a}_{\mathbf{k}\sigma}^{n\dagger} = \frac{1}{\sqrt{N}} \sum_{i\alpha} C_{\alpha\sigma}^n(\mathbf{k})^* e^{-i\mathbf{k}\cdot\mathbf{R}_i} \hat{c}_{i\alpha\sigma}^\dagger.$$

Here $C_{\alpha}^n(\mathbf{k}\sigma)$ are the expansion coefficients of Bloch states in terms of localized orbitals, N the number of unit cells. H^H becomes

$$\begin{aligned} \hat{H}^H = & \sum_{\mathbf{k}n\sigma} \epsilon_{\mathbf{k}n\sigma}^H \hat{a}_{\mathbf{k}\sigma}^{n\dagger} \hat{a}_{\mathbf{k}\sigma}^n + \sum_{\alpha\beta} \sum_{\mathbf{k}\mathbf{k}'\mathbf{p}} \sum_{nn'} \sum_{mm'} \sum_{\sigma} \frac{1}{2N} \\ & \times [U_{\alpha\beta} C_{\alpha\sigma}^n(\mathbf{k})^* C_{\alpha\sigma}^{n'}(\mathbf{k}+\mathbf{p}) C_{\beta-\sigma}^m(\mathbf{k}')^* \\ & \times C_{\beta-\sigma}^{m'}(\mathbf{k}'-\mathbf{p}) \hat{a}_{\mathbf{k}\sigma}^{n\dagger} \hat{a}_{\mathbf{k}+\mathbf{p}\sigma}^{n'} \hat{a}_{\mathbf{k}'-\sigma}^{m\dagger} \hat{a}_{\mathbf{k}'-\sigma}^{m'} \\ & + (U_{\alpha\beta} - J_{\alpha\beta}) C_{\alpha\sigma}^n(\mathbf{k})^* C_{\alpha\sigma}^{n'}(\mathbf{k}+\mathbf{p}) \\ & \times C_{\beta\sigma}^m(\mathbf{k}')^* C_{\beta\sigma}^{m'}(\mathbf{k}'-\mathbf{p}) \hat{a}_{\mathbf{k}\sigma}^{n\dagger} \hat{a}_{\mathbf{k}+\mathbf{p}\sigma}^{n'} \hat{a}_{\mathbf{k}'\sigma}^{m\dagger} \hat{a}_{\mathbf{k}'-\mathbf{p}\sigma}^{m'}]. \end{aligned} \quad (2.6)$$

Now $\epsilon_{\mathbf{k}n\sigma}^H$ includes also the kinetic part of the single-particle Hamiltonian and the Coulomb and exchange integrals are assumed to be site independent. In the same way H^{MF} becomes

$$\hat{H}^{\text{MF}} = \sum_{\mathbf{k}n\sigma} \epsilon_{\mathbf{k}n\sigma}^{\text{MF}} \hat{a}_{\mathbf{k}\sigma}^{n\dagger} \hat{a}_{\mathbf{k}\sigma}^n, \quad (2.7)$$

with

$$\epsilon_{\mathbf{k}n\sigma}^{\text{MF}} = \epsilon_{\mathbf{k}n\sigma}^H + Q_{\mathbf{k}\sigma}^n, \quad (2.8)$$

$$\begin{aligned} Q_{\mathbf{k}\sigma}^n = & \sum_{\alpha\beta} |C_{\alpha\sigma}^n(\mathbf{k})|^2 \left[U_{\alpha\beta} \frac{1}{N} \sum_{\mathbf{k}'n'}^{\text{occ}} |C_{\beta-\sigma}^{n'}(\mathbf{k}')|^2 \right. \\ & \left. + (U_{\alpha\beta} - J_{\alpha\beta}) \frac{1}{N} \sum_{\mathbf{k}'n'}^{\text{occ}} |C_{\beta\sigma}^{n'}(\mathbf{k}')|^2 \right], \end{aligned} \quad (2.9)$$

which is the analog of Eq. (2.4) for Bloch states. Notice that the sums over n' are over occupied states. Equations (2.8) and (2.9) contain the correct recipe to include Hubbard correlation starting from band structure eigenvalues $\epsilon_{\mathbf{k}n\sigma}^{\text{MF}}$ and are essential in order to avoid double counting of e - e interaction.

III. HOLE SPECTRAL FUNCTION, SELF-ENERGY, AND THE FADDEEV METHOD

We are interested in the hole spectral function

$$D_{\mathbf{k}\sigma}^-(\omega) = -\frac{1}{\pi} \sum_n \text{Im} \mathcal{G}^-(\mathbf{k}n\sigma, \omega), \quad (3.1)$$

which is the quantity directly related to the photoemission results we want to compare with. It describes the removal of one electron of wave vector \mathbf{k} , band index n , and spin σ and is related to the hole propagator

$$\begin{aligned} \mathcal{G}^-(\mathbf{k}n\sigma, \omega) = & -\langle \Psi_0 | \hat{a}_{\mathbf{k}\sigma}^{n\dagger} \hat{G}(z) \hat{a}_{\mathbf{k}\sigma}^n | \Psi_0 \rangle, \\ z = & -\omega + E_0(N_e) + i\delta \end{aligned} \quad (3.2)$$

$E_0(N_e)$ and $|\Psi_0\rangle$ define the ground state of the N_e -particle system and

$$\hat{G}(z) = \frac{1}{z - \hat{H}^H} \quad (3.3)$$

is the resolvent operator. The hole propagator can also be written in terms of the hole self-energy as

$$\mathcal{G}^-(\mathbf{k}n\sigma, \omega) = \frac{1}{\omega - \epsilon_{\mathbf{k}n\sigma}^{\text{MF}} - \Sigma_{\mathbf{k}n\sigma}^-(\omega)}, \quad (3.4)$$

where $\Sigma_{\mathbf{k}n\sigma}^-(\omega)$ is the self-energy correction to *band* eigenvalues $\epsilon_{\mathbf{k}n\sigma}^{\text{MF}}$. In order to calculate $\Sigma_{\mathbf{k}n\sigma}^-(\omega)$ we proceed as in Ref. 6 adopting a configuration-interaction scheme which consists in projecting the Hubbard Hamiltonian on a set of states obtained by adding a finite number of e - h pairs to the Fermi sea, i.e., to the ground state $|\Phi_0\rangle$ of the single-particle Hamiltonian. We will adopt the three-body scattering approach where this expansion is truncated to include just one e - h pair: the state with one removed electron of momentum \mathbf{k} and spin σ is expanded in terms of the basis set including one-hole configurations and three-particle configurations (one hole plus one e - h pair) we will denote by $|s\rangle$ and $|t\rangle$, respectively,

$$|s\rangle \equiv \hat{a}_{\mathbf{k}n\sigma} |\Phi_0\rangle, \quad |t\rangle \equiv \hat{a}_{\mathbf{q}_3 n_3 \sigma_3}^\dagger \hat{a}_{\mathbf{q}_2 n_2 \sigma_2} \hat{a}_{\mathbf{q}_1 n_1 \sigma_1} |\Phi_0\rangle, \quad (3.5)$$

with

$$\mathbf{q}_1 + \mathbf{q}_2 - \mathbf{q}_3 = \mathbf{k}, \quad \sigma_1 + \sigma_2 - \sigma_3 = \sigma.$$

To be consistent the basis set for the N_e -particle interacting system will include zero- and two-particle configurations. The ground state of the interacting N_e -particle system coincides then with the noninteracting one; this is obvious for the single-band Hamiltonian discussed in Ref. 6 (the state with zero and one e - h pair added coincide due to k -vector conservation) and still holds in the present case of multiband Hamiltonian since H^H has no off-diagonal matrix elements among two-particle configurations. As a consequence in the 3BS approximation the hole propagator is the average of the resolvent over states $|s\rangle$.

By projecting the Hamiltonian (2.6) over the complete set appropriate for the $(N_e - 1)$ -particle system we get an approximate expression for \hat{H}^H appropriate to describe one-electron removal,

$$\hat{H}_{N_e-1}^H \simeq \hat{H}_1 + \hat{H}_3 + \hat{V}. \quad (3.6)$$

Here \hat{H}_1 is associated to one-hole configurations,

$$\hat{H}_1 = \langle s | \hat{H}^H | s \rangle \langle s |,$$

\hat{H}_3 describes the contribution of three-particle configurations,

$$\hat{H}_3 = \sum_{tt'} \langle t | \hat{H}^H | t' \rangle | t \rangle \langle t' |,$$

and \hat{V} is the coupling between one- and three-particle states,

$$\hat{V} = \sum_t \langle s | \hat{H}^H | t \rangle | s \rangle \langle t | + \text{H.c.}$$

We leave the detailed expression of the matrix elements of the multiband \hat{H}^H to Appendix A and proceed to sketch the method for the calculation of the resolvent (3.3). We define the three-particle resolvent, that is, the resolvent associated to the three-particle interaction

$$\hat{F}_3(z) = \frac{1}{z - \hat{H}_3}$$

and the Dyson equation which relates $\hat{G}(z)$ to it,

$$\hat{G}(z) = \hat{F}_3(z) + \hat{F}_3(z) [\hat{H}_1 + \hat{V}] \hat{G}(z). \quad (3.7)$$

It is a matter of simple algebra to show that the hole propagator can then be expressed in terms of \hat{F}_3 as

$$\begin{aligned} \mathcal{G}^-(\mathbf{k}n\sigma, \omega) &= -G_{ss}(z) \\ &= \frac{1}{\omega - E_0(N_e) + H_{ss}^H + \sum_{tt'} F_{3tt'} V_{t's} V_{st}}, \end{aligned} \quad (3.8)$$

with the notation $G_{ss} \equiv \langle s | \hat{G} | s \rangle$, $F_{3tt'} \equiv \langle t | \hat{F}_3 | t' \rangle$, etc. Since the difference between the ground state energy of the N_e -particle system $E_0(N_e)$ and the average of H^H over $|s\rangle$ states turns out to be

$$E_0(N_e) - H_{ss}^H = \epsilon_{\mathbf{k}n\sigma}^H + Q_{\mathbf{k}\sigma}^n = \epsilon_{\mathbf{k}n\sigma}^{\text{MF}}$$

the band eigenvalues appear naturally in the denominator of the hole propagator and, comparing Eq. (3.8) with Eq. (3.4), we can identify the self-energy correction to band eigenvalues we are interested in as

$$\Sigma^-(\mathbf{k}n\sigma, \omega) = - \sum_{tt'} F_{3tt'} V_{t's} V_{st}. \quad (3.9)$$

The determination of the hole propagator is then reduced to the calculation of $F_{3tt'}$. This is done according to the Faddeev scattering theory²⁴ as described for the single-band case in Ref. 6. The method consists in separating the three-body Hamiltonian in diagonal and nondiagonal parts

$$\hat{H}_3^D = \sum_t \langle t | \hat{H}^H | t \rangle | t \rangle \langle t |,$$

$$\hat{H}_3^{\text{ND}} = \sum_{tt'} \langle t | \hat{H}^H | t' \rangle | t \rangle \langle t' |,$$

defining the diagonal three-body resolvent

$$\hat{F}_3^D(z) = \frac{1}{z - \hat{H}_3^D}$$

and the scattering operator

$$\hat{S} = \hat{H}_3^{\text{ND}} + \hat{H}_3^{\text{ND}} \hat{F}_3^D \hat{S}.$$

The three-body resolvent can then be written as

$$\hat{F}_3 = \hat{F}_3^D + \hat{F}_3^D \hat{S} \hat{F}_3^D. \quad (3.10)$$

As shown in Appendix A and Ref. 6 the nondiagonal three-body interaction is the sum of two potentials,

$$\hat{H}_3^{\text{ND}} = \hat{V}_{h-h} + \hat{V}_{h-e},$$

which describe $h-h$ and $h-e$ multiple scattering.

We define partial scattering operators

$$\hat{S}_{h-h} = \hat{V}_{h-h} + \hat{H}_{h-h} \hat{F}_3^D \hat{S},$$

$$\hat{S}_{h-e} = \hat{V}_{h-e} + \hat{H}_{h-e} \hat{F}_3^D \hat{S}$$

which are related to the scattering T matrices,

$$\hat{T}_{h-h} = \hat{V}_{h-h} + \hat{V}_{h-h} \hat{F}_3^D \hat{T}_{h-h}, \quad (3.11a)$$

$$\hat{T}_{h-e} = \hat{V}_{h-e} + \hat{V}_{h-e} \hat{F}_3^D \hat{T}_{h-e}, \quad (3.11b)$$

through

$$\hat{S}_{h-h} = \hat{T}_{h-h} + \hat{T}_{h-h} \hat{F}_3^D \hat{S}_{h-e}, \quad (3.12a)$$

$$\hat{S}_{h-e} = \hat{T}_{h-e} + \hat{T}_{h-e} \hat{F}_3^D \hat{S}_{h-h}. \quad (3.12b)$$

These are the Faddeev equations which must be solved in order to get $\hat{S} = \hat{S}_{h-h} + \hat{S}_{h-e}$, \hat{F}_3 from Eq. (3.10), and $\mathcal{G}^-(\mathbf{k}n\sigma, \omega)$ from Eq. (3.8). Inserting Eq. (3.12) into Eq. (3.10) one gets the expression for the three-particle resolvent in terms of scattering operators S_{h-e} and T_{h-h} ,

$$\hat{F}_3 = \hat{F}_3^D + \hat{F}_3^D (\hat{T}_{h-h} + \hat{T}_{h-h} \hat{F}_3^D \hat{S}_{h-e} + S_{h-e}) \hat{F}_3^D. \quad (3.13)$$

Further steps are necessary in order to make this general method practical for real calculations — and further approximations as well. In the following we will specialize to valence and core states.

IV. VALENCE STATES

We adopt some simplifying assumptions for the description of photoemission from valence states of nickel. We will consider $e-e$ correlation among d electrons only and neglect the orbital dependence of one-center integrals involving valence d electrons; we set

$$U_{\alpha\beta} = \begin{cases} U_{vv} & \text{for } \alpha, \beta = d \text{ orbitals} \\ 0 & \text{elsewhere} \end{cases}$$

and similarly for the exchange parameter $J_{\alpha\beta}$; moreover we will neglect $U_{vv} - J_{vv}$ with respect to U_{vv} . In this way the Hamiltonian (2.6) reduces to

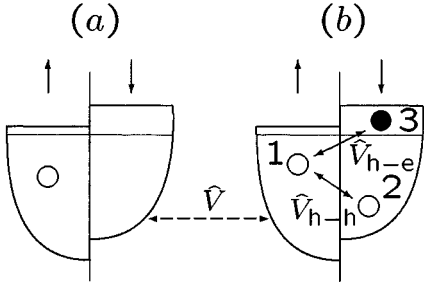


FIG. 1. Schematic representation of the basis set for the configuration expansion of the interacting state with one electron removed from the majority-spin band. \hat{V} , \hat{V}_{h-h} , \hat{V}_{h-e} describe the coupling between one- and three-particle states, the hole-hole, and the hole-electron interaction, respectively.

$$\begin{aligned} \hat{H}^H = & \sum_{\mathbf{k}n\sigma} \epsilon_{\mathbf{k}n\sigma}^H \hat{a}_{\mathbf{k}\sigma}^{n\dagger} \hat{a}_{\mathbf{k}\sigma}^n \\ & + \sum_{\alpha\beta} U_{\alpha\beta} \sum_{\mathbf{k}\mathbf{k}'\mathbf{p}} \sum_{nn'} \sum_{mm'} \sum_{\sigma} \frac{1}{2N} C_{\alpha\sigma}^n(\mathbf{k})^* \\ & \times C_{\alpha\sigma}^{n'}(\mathbf{k}+\mathbf{p}) C_{\beta-\sigma}^m(\mathbf{k}')^* C_{\beta-\sigma}^{m'}(\mathbf{k}'-\mathbf{p}) \\ & \times \hat{a}_{\mathbf{k}\sigma}^{n\dagger} \hat{a}_{\mathbf{k}+\mathbf{p}\sigma}^{n'} \hat{a}_{\mathbf{k}'-\sigma}^{m\dagger} \hat{a}_{\mathbf{k}'-\mathbf{p}-\sigma}^{m'}. \end{aligned} \quad (4.1)$$

Finally we will exclude configurations with e - h pair added to the majority-spin band as it would be strictly correct in the strong ferromagnetic limit where no empty states are available in the majority-spin band.

The states which define the basis set for the $N_e - 1$ system are schematically illustrated in Fig. 1; the nonzero interaction potentials responsible for h - h and e - h scattering are also indicated. Notice that holes and electrons of parallel spin do not interact due to the assumption $U_{vv} - J_{vv} \simeq 0$.

We have already stressed that the Hubbard correlation enters the definition of quasiparticle energies twice: first as a mean-field correction to *bare* eigenvalues, transforming them into *band* ones according to Eq. (2.8); second through the addition of self-energy (3.9). The calculation of this last quantity requires a generalization of the method illustrated in detail in Ref. 6 for the much simpler case of a single-band Hamiltonian. The situation here is complicated by the sums over orbital indices appearing in the effective Hamiltonian. This requires the definition of orbital-dependent diagonal Green functions and T matrices as described in Appendix B. As a result the self-energy correction to a band eigenvalue of wave vector \mathbf{k} , spin σ , and band index n turns out to depend on the quantum numbers n and \mathbf{k} as

$$\begin{aligned} \Sigma_{\mathbf{k}n\sigma}^-(\omega) = & \sum_{\beta} |C_{\beta\sigma}^n(\mathbf{k})|^2 \left[\sum_{\alpha} U_{\alpha\beta} \frac{1}{N} \sum_{\mathbf{k}'}^{\text{empty}} |C_{\alpha-\sigma}^{n'}(\mathbf{k}')|^2 \right. \\ & \left. - \Sigma_{\beta\sigma}(\omega) \right]. \end{aligned} \quad (4.2)$$

The k -vector and band-index dependence of self-energy is associated to the local orbital coefficients which modulate an orbital self-energy

$$\begin{aligned} \Sigma_{\beta\sigma}^-(\omega) = & \sum_{\alpha} \int_{E_f}^{\infty} d\epsilon n_{\alpha-\sigma}(\epsilon) T_{h-h}^{\alpha\beta}(\omega-\epsilon) \\ & \times [1 + U_{\alpha\beta} A^{\alpha\beta}(\omega-\epsilon)], \end{aligned} \quad (4.3)$$

where $n_{\alpha\sigma}(\epsilon)$ is the spin-dependent orbital density of d valence states and $T_{h-h}^{\alpha\beta}$ is the orbital-dependent t matrix describing the hole-hole multiple scattering,

$$T_{h-h}^{\alpha\beta}(\omega) = \frac{U_{\alpha\beta}}{1 + U_{\alpha\beta} \mathcal{G}_3^{\alpha\beta}(\omega)}, \quad (4.4)$$

with

$$g_3^{\alpha\beta}(\omega) = \int_{-\infty}^{E_f} d\epsilon' \int_{-\infty}^{E_f} d\epsilon \frac{n_{\alpha-\sigma}(\epsilon) n_{\beta}(\epsilon')}{\omega - \epsilon' - \epsilon - i\delta}. \quad (4.5)$$

$A^{\alpha\beta}$ includes the hole-electron scattering; it is determined by solving the integral equation

$$\begin{aligned} A^{\alpha\beta}(\omega, \epsilon) = & B^{\alpha\beta}(\omega, \epsilon) + \int_{E_f}^{\infty} d\epsilon' n_{\alpha-\sigma}(\epsilon') \\ & \times K^{\alpha\beta}(\omega, \epsilon, \epsilon') A^{\alpha\beta}(\omega, \epsilon'), \end{aligned} \quad (4.6)$$

where

$$\begin{aligned} K^{\alpha\beta}(\omega, \epsilon, \epsilon') = & \int_{-\infty}^{E_f} d\epsilon'' n_{\alpha-\sigma}(\epsilon'') g_2^{\beta}(\omega + \epsilon'' - \epsilon) T_{h-e}^{\alpha\beta} \\ & \times (\omega + \epsilon'') g_2^{\beta}(\omega + \epsilon'' - \epsilon') T_{h-h}^{\alpha\beta}(\omega - \epsilon''), \end{aligned} \quad (4.7)$$

$$\begin{aligned} B^{\alpha\beta}(\omega, \epsilon) = & \int_{-\infty}^{E_f} d\epsilon' n_{\alpha-\sigma}(\epsilon') g_2^{\beta}(\omega + \epsilon' - \epsilon) T_{h-e}^{\alpha\beta} \\ & \times (\omega + \epsilon') \left(g_1^{\alpha\beta}(\omega - \epsilon') + \int_{E_f}^{\infty} d\epsilon'' n_{\alpha-\sigma}(\epsilon'') \right. \\ & \left. \times g_2^{\beta}(\omega + \epsilon' - \epsilon'') g_3^{\alpha\beta}(\omega - \epsilon'') T_{h-h}^{\alpha\beta}(\omega - \epsilon'') \right). \end{aligned} \quad (4.8)$$

$T_{h-e}^{\alpha\beta}$ is the orbital-dependent t matrix describing the hole-electron scattering,

$$T_{h-e}^{\alpha\beta}(\omega) = \frac{-U_{\alpha\beta}}{1 - U_{\alpha\beta} \mathcal{G}_1^{\alpha\beta}(\omega)}, \quad (4.9)$$

with

$$g_1^{\alpha\beta}(\omega) = \int_{-\infty}^{E_f} d\epsilon' \int_{E_f}^{\infty} d\epsilon \frac{n_{\alpha-\sigma}(\epsilon) n_{\beta\sigma}(\epsilon')}{\omega - \epsilon' + \epsilon - i\delta} \quad (4.10)$$

and finally

$$g_2^{\beta}(\omega) = \int_{-\infty}^{E_f} d\epsilon' \frac{n_{\beta\sigma}(\epsilon')}{\omega - \epsilon' - i\delta}. \quad (4.11)$$

Equations (4.2)–(4.11) describe the procedure we have followed to calculate in practice self-energy corrections for the valence states of Ni reported in Sec. VI.

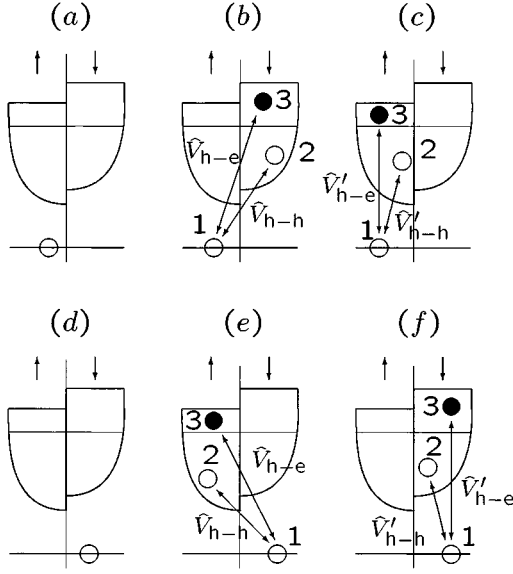


FIG. 2. Schematic representation of the basis set for the configuration expansion of core states.

V. CORE STATES

The localized character of core states is responsible for much stronger correlation effects associated with larger on-site Coulomb and exchange integrals. In order to adapt the Hamiltonian (2.6) to the case of core states we make the following assumptions: we neglect the correlation among valence electrons and assume them to be described by a single band. In Eq. (2.6) the band index n can have just two values as does the orbital index and we are left with a two-band Hamiltonian

$$\hat{H}^H = \hat{H}_{vv} + \hat{H}_{cc} + \hat{H}_{cv}, \quad (5.1)$$

where \hat{H}_{vv} is the band Hamiltonian for valence electrons with the $e-e$ interaction treated in the mean-field approximation,

$$\hat{H}_{vv} = \sum_{\mathbf{k}\sigma} \epsilon_{\mathbf{k}\sigma}^{\text{MF}} \hat{a}_{\mathbf{k}\sigma}^\dagger \hat{a}_{\mathbf{k}\sigma}$$

and

$$\begin{aligned} \hat{H}_{cc} = & \sum_{\mathbf{k}\sigma} \epsilon_{\mathbf{k}\sigma}^H \hat{a}_{\mathbf{k}\sigma}^\dagger \hat{a}_{\mathbf{k}\sigma} \\ & + \sum_{\mathbf{k}\mathbf{k}'\mathbf{p}} \sum_{\sigma} \frac{U_{cc}}{N} \hat{a}_{\mathbf{k}\sigma}^\dagger \hat{a}_{\mathbf{k}+\mathbf{p}\sigma} \hat{a}_{\mathbf{k}'-\sigma}^\dagger \hat{a}_{\mathbf{k}'-\mathbf{p}\sigma}, \end{aligned}$$

$$\begin{aligned} \hat{H}_{cv} = & \sum_{\mathbf{k}\mathbf{k}'\mathbf{p}} \sum_{\sigma} \frac{1}{N} [U_{cv} C_{v-\sigma}(\mathbf{k}')^* C_{v-\sigma}(\mathbf{k}'-\mathbf{p}) \\ & \times \hat{a}_{\mathbf{k}\sigma}^\dagger \hat{a}_{\mathbf{k}+\mathbf{p}\sigma} \hat{a}_{\mathbf{k}'-\sigma}^\dagger \hat{a}_{\mathbf{k}'-\mathbf{p}\sigma} + (U_{cv} - J_{cv}) \\ & \times C_{v\sigma}(\mathbf{k}')^* C_{v\sigma}(\mathbf{k}'-\mathbf{p}) \hat{a}_{\mathbf{k}\sigma}^\dagger \hat{a}_{\mathbf{k}+\mathbf{p}\sigma} \hat{a}_{\mathbf{k}'-\sigma}^\dagger \hat{a}_{\mathbf{k}'-\mathbf{p}\sigma}]. \end{aligned}$$

Here $U_{cc} = J_{cc}$, U_{cv} , and J_{cv} describe the interactions between core-core and core-valence d electrons.

Figure 2 shows schematically the configurations to be in-

cluded for the 3BS description. Notice that configurations with one $e-h$ pair added to the majority-spin band are now considered: even if the number of empty states available is small, the stronger value of the interactions makes these scattering channels no longer negligible. As shown in Fig. 2 we have then to take into account scattering between particles of parallel spin proportional to $U_{cv} - J_{cv}$ and between particles of opposite spin proportional to U_{cv} . The extra configurations where all the particles (holes and electrons) have the same spin are called $|z\rangle$.

The procedure to calculate self-energy for core states is a straightforward extension of the one outlined for valence states. The core hole propagator turns out to be given by

$$\mathcal{G}^-(\mathbf{k}c\sigma, \omega) = \frac{1}{\omega - \epsilon_{c\sigma}^{\text{MF}} - \sum_{tt'} F_{3tt'} V_{t's} V_{st} - \sum_{zz'} F_{3zz'} V_{z's} V_{sz}}. \quad (5.2)$$

The presence here of extra configurations and extra interactions does not imply any major difference with respect to the case of valence states — just the addition of an extra term in the denominator of Eq. (5.2) and the necessity to solve separately two Faddeev problems to calculate $F_{3tt'}$ and $F_{3zz'}$ for opposite and parallel spin interactions, respectively. This is a consequence of the fact that the Hamiltonian (5.1) does not mix $|z\rangle$ and $|t\rangle$ configurations. The Faddeev problem for the determination of $F_{3zz'}$ is solved in the same way as described in Appendix B for $F_{3tt'}$, substituting U_{cv} with $U_{cv} - J_{cv}$ and parallel spin instead of opposite ones. Moreover the description of the core state in terms of a zero-width band with a δ function as orbital density of states drastically reduces the computational effort required to evaluate the noninteracting Green functions (4.5), (4.10), and (4.11).

The relationship between the energy $\epsilon_{c\sigma}^{\text{MF}}$ and the bare core eigenvalue involves as usual $Q_{\mathbf{k}\sigma}^n$ [see Eqs. (2.8) and (2.9)]; explicitly one has

$$\epsilon_{c\sigma}^{\text{MF}} = \epsilon_{c\sigma}^H + [(U_{cv} - J_{cv}) \langle \hat{n}_{v\sigma} \rangle + U_{cv} \langle \hat{n}_{v-\sigma} \rangle] + U_{cc} \langle \hat{n}_{c-\sigma} \rangle. \quad (5.3)$$

It is interesting to make a comment concerning the role of the Coulomb repulsion U_{cc} . Since any three-particle (one hole plus one $e-h$ pair) configuration must involve empty states, no multiple scattering is associated with U_{cc} and this quantity gives rise just to a mean-field contribution. Core-valence interactions U_{cv} and J_{cv} on the contrary modify the bare core energies both through the mean-field contribution and by self-energy corrections which originate from hole-hole and electron-hole scattering of opposite and parallel spin described by $F_{3tt'}$ and $F_{3zz'}$, respectively.

VI. RESULTS

The calculation of self-energy corrections requires as an input (i) the mean-field eigenvalues and eigenvectors for valence electrons, (ii) the energy of the core level, and (iii) the values of the Coulomb and exchange parameters U_{vv} , U_{cc} , U_{cv} , J_{cv} . All these quantities can in principle be deduced from an *ab initio* density functional calculation; Coulomb integrals in particular can be obtained in the so-called

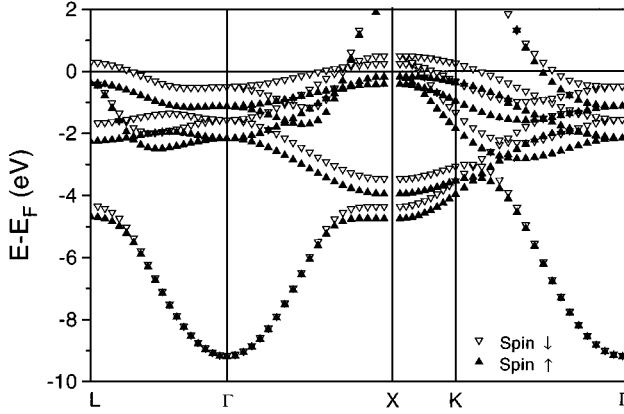


FIG. 3. Single-particle band structure of nickel obtained using the LMTO method. Energies are referred to the Fermi energy. Open triangles, minority-spin states; filled triangles, majority-spin states.

constrained-density functional scheme²⁵ — a procedure which is, however, not free of ambiguities (see, for instance, the discussion reported in Ref. 13) and can lead to large variations in the estimated values. We have therefore adopted a mixed strategy, using results of *ab initio* band calculations to get quantities (i) only, treating all the others as free parameters.

The band structure of ferromagnetic nickel has been calculated with the linear muffin-tin orbital (LMTO) method in the atomic-spheres approximation (ASA) including the combined correction term.²⁶ The tight-binding LMTO basis set²⁷ has been used, including nine orbitals (*s*, *p*, *d*) per atom. The resulting energy dispersion is shown in Fig. 3; the occupation numbers for valence *d* orbitals turn out to be $\langle n_{v\uparrow} \rangle = 4.68$, $\langle n_{v\downarrow} \rangle = 4.07$. We have used the single-particle eigenvalues and the corresponding *d* contribution to eigenfunctions and orbital densities of states to calculate self-energy corrections and spectral functions according to the theory described in the previous sections. A value of $U_{vv} = 2$ eV has been chosen in order to reproduce the observed energy position of the valence band satellite; as we will show below we are able in this way to reproduce also other characteristics of the valence quasiparticle states such as bandwidth, quasiparticle energy dispersion, and exchange splitting; this is an important result and represents a success of the present approach: previous methods based on a simplified description of the scattering channels^{14,15} in fact have not been able to reproduce at the same time the satellite energy position and the valence band width which turned out to be systematically overestimated for values of the Coulomb integral fixed to reproduce the satellite binding energy.

Figure 4 shows the comparison between our results and recent angle-integrated/spin-resolved photoemission data.³ We find that the calculated total spectral function $D_{\sigma}^{-}(\omega)$ defined as

$$D_{\sigma}^{-}(\omega) = \sum_{\mathbf{k}\ell} D_{\mathbf{k}\ell\sigma}^{-}(\omega)$$

closely reproduces the experimental energy distribution curves for each spin component; notice in particular that the 6 eV satellite is observed clearly only in the photoemission

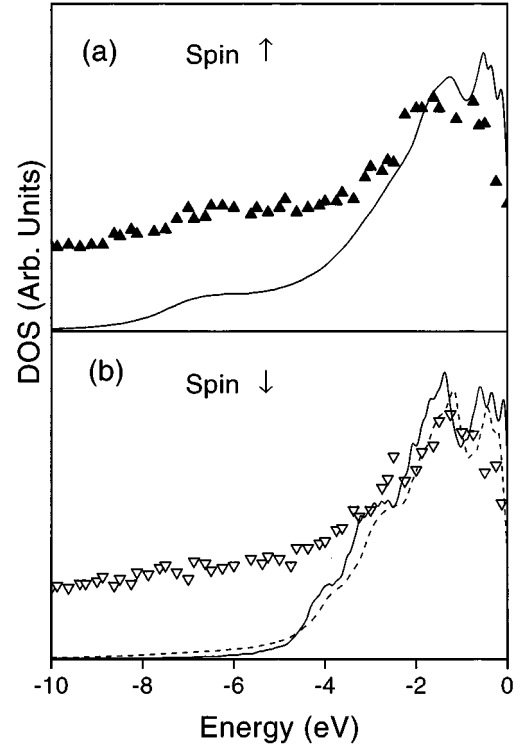


FIG. 4. Density of quasiparticle states of nickel for majority spin (a) and minority spin (b) compared with experimental results of angle-integrated spin-resolved photoemission results (filled triangles) of Ref. 3. The results for minority-spin bands obtained without the strong-ferromagnetic-limit approximation are shown as a broken line in panel (b).

from majority-spin states in agreement with our results. The two approximations we have adopted for the description of valence states, that is, $U_{vv} - J_{vv} \approx 0$ and the strong ferromagnetic limit, make the self-energy corrections exactly zero for minority-spin bands and the comparison between our results and the spin-resolved experimental data confirms the validity of both these assumptions. As a further evidence of this we report in Fig. 4 the minority-spin spectral function calculated after removing the assumption of strong ferromagnetism, i.e., considering also *e-h* pairs added to the majority-spin band; the small number of empty states and the relatively small value of the interaction U_{vv} make these scattering channels not efficient and the calculated spectrum is not significantly altered.

It is possible to perform a more refined analysis by looking at the *k*-resolved spectral function; Fig. 5(a) shows the spectral function for the *K* point and $\epsilon_{\mathbf{k}\ell\uparrow}^{\text{MF}} = -3.6$ eV together with the corresponding self-energy $\Sigma_{\mathbf{k}\ell\uparrow}^{-}(\omega)$. The spectral function shows a quasiparticle peak plus a satellite: the first structure is associated to the pole of the hole propagator shown in Fig. 5(b) as the interception between $\text{Re}[\Sigma_{\mathbf{k}\ell\uparrow}^{-}(\omega)]$ and the straight line $\omega - \epsilon_{\mathbf{k}\ell\uparrow}^{\text{MF}}$. The second structure is associated to the maximum of $\text{Im}[\Sigma_{\mathbf{k}\ell\uparrow}^{-}(\omega)]$ and as such it will occur at the same energy at any *k* vector. This appears more clearly by extending the same analysis to the *k* points along the high symmetry line of the Brillouin zone and plotting the energy position of the maxima of $D_{\mathbf{k}\sigma}^{-}(\omega) = \sum_n D_{\mathbf{k}\ell n\sigma}^{-}(\omega)$ to get the quasiparticle band structure

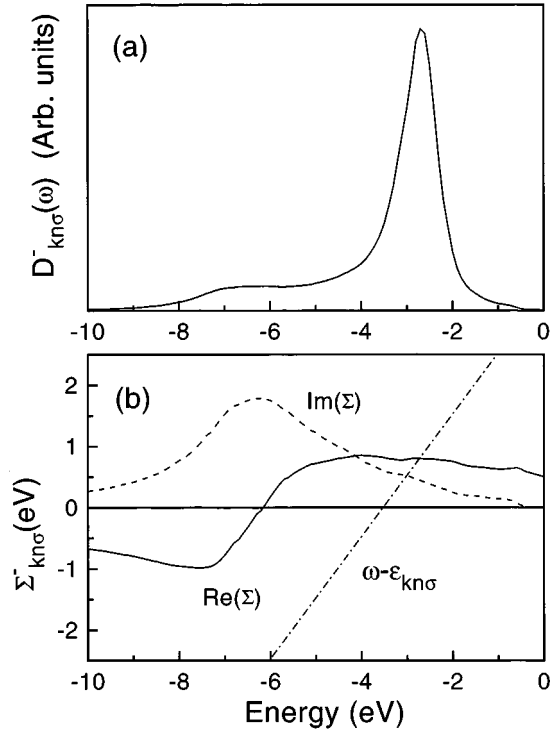


FIG. 5. Spectral function (a) and self-energy (b) for the K point and $\epsilon_{kn\uparrow}^{\text{MF}} = -3.6$ eV. The interception between $\text{Re}[\Sigma^-(kn\uparrow, \omega)]$ and the straight line $\omega - \epsilon_{kn\uparrow}^{\text{MF}}$ indicate the position of the quasiparticle pole.

of Fig. 6. By comparing the quasiparticle band structure with the single-particle results it appears that the majority-spin eigenvalues are heavily affected by self-energy corrections, showing a strong reduction of the d -band width and the presence of the above mentioned 6 eV satellite. Since the majority-spin eigenvalues are shifted to lower binding energies while the minority-spin ones are unaffected, the splitting between majority and minority states becomes smaller than in the original single-particle bands. This goes in the right direction since it is well known that single-particle calculations overestimate this quantity; from Fig. 6 it appears that

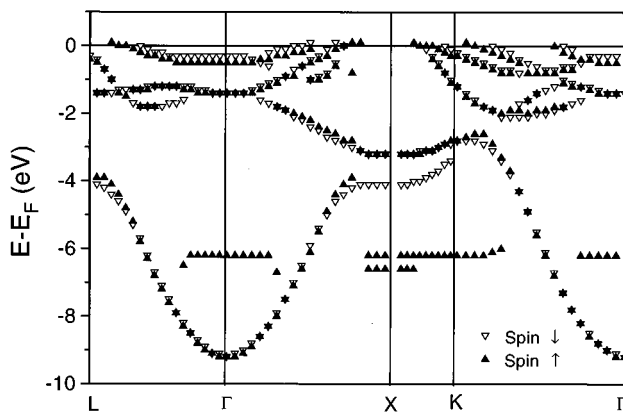


FIG. 6. Quasiparticle band structure of nickel along the high symmetry directions of the Brillouin zone. Energies are referred to the Fermi energy. Open triangles, minority-spin states; filled triangles, majority-spin states.

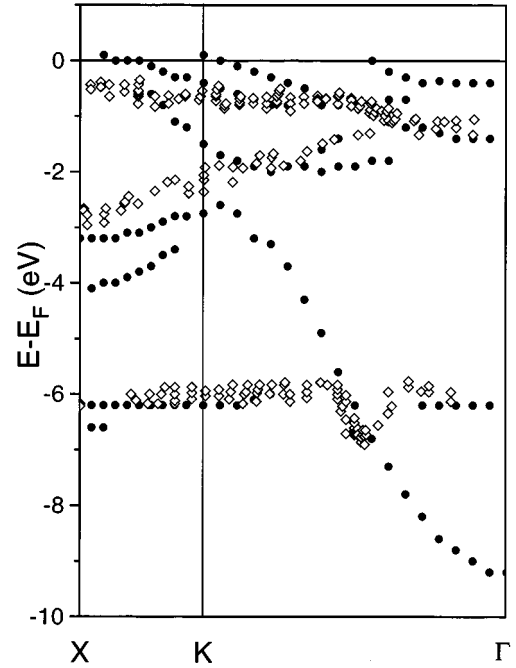


FIG. 7. Comparison between the calculated dispersion of hole quasiparticle states (circles) for majority-spin bands and angle-resolved spin-integrated photoemission results (diamonds) of Ref. 29.

the energy separation between majority and minority quasiparticle peaks around the Γ point is 0.2 eV for the topmost band. This result is in remarkable agreement with a recent estimate reporting a split of 204 ± 8 meV along the Σ direction.²⁸ The same is true for the quasiparticle energy dispersion as a whole, which is shown in Fig. 7 compared with the results of angle-resolved spin-integrated photoemission spectroscopy of Ref. 29.

As far as core levels are concerned we consider here the $3p$ level of nickel as a test case. Since the core levels of an isolated atom are degenerate in spin their spin dependence is a solid state effect, associated to the interaction between the atom and the solid it is embedded in; in other words the spin dependence of core-level energies is related to the spin polarization of the valence band on one side and to core-valence interactions on the other. According to our view the relevant quantities are the Coulomb and exchange integrals between core and valence orbitals which affect the bare atomic core energies both through the mean-field term $Q_{k\sigma}^n$ and self-energy corrections. The mean-field contribution of Eq. (5.3) gives rise to a spin splitting proportional to J_{cv} and to the valence band spin polarization

$$\epsilon_{c\uparrow}^{\text{MF}} - \epsilon_{c\downarrow}^{\text{MF}} = J_{cv} (\langle \hat{n}_{v\downarrow} \rangle - \langle \hat{n}_{v\uparrow} \rangle).$$

Notice that U_{cv} and U_{cc} do not enter this expression; they affect the bare core level $\epsilon_{c\uparrow}^H = \epsilon_{c\downarrow}^H$ according to

$$\epsilon_{c\uparrow}^H + [U_{cv} (\langle \hat{n}_{v\uparrow} \rangle + \langle \hat{n}_{v\downarrow} \rangle) + U_{cc} \langle \hat{n}_{c\downarrow} \rangle] \equiv \epsilon_c, \quad (6.1)$$

TABLE I. Parameters used in the calculations of Ni 3*p* core hole spectrum.

U_{cv}	J_{cv}	$\epsilon_c^{1/2}$	$\epsilon_c^{3/2}$
5.00 eV	2.50 eV	-59.00 eV	-57.50 eV

giving rise to a modified core energy level ϵ_c which is still spin independent. The mean-field eigenvalues are related to this quantity as

$$\epsilon_{c\sigma}^{\text{MF}} = \epsilon_c - J_{cv} \langle \hat{n}_{v\sigma} \rangle.$$

We have used spin-orbit split values of ϵ_c , that is, $\epsilon_c^{3/2}$ and $\epsilon_c^{1/2}$, to fix the absolute value of the core-level binding energy, choosing then J_{cv} to reproduce the spin splitting of the main peak observed in the core-level photoemission.³ The last parameter, that is, U_{cv} , has been fixed in order to reproduce the satellite's energy position. The values which optimize the agreement between our calculation and the experimental results are listed in Table I.

Figure 8 shows the calculated self-energy for the creation of both majority- and minority-spin hole in the core level $3p^{1/2}$. The same analysis obviously applies to the other spin-orbit split level $3p^{3/2}$. In the case of the minority-spin core hole the self-energy presents two well defined structures: the one at lower binding energy is related to the scattering between particles of parallel spin with strength proportional to $U_{cv} - J_{cv}$ [see Fig. 2(f)] while the structure at higher binding energy is related to U_{cv} and to the scattering between opposite spin particles [see Fig. 2(e)]. Notice that two independent factors determine the efficiency of the scattering pro-

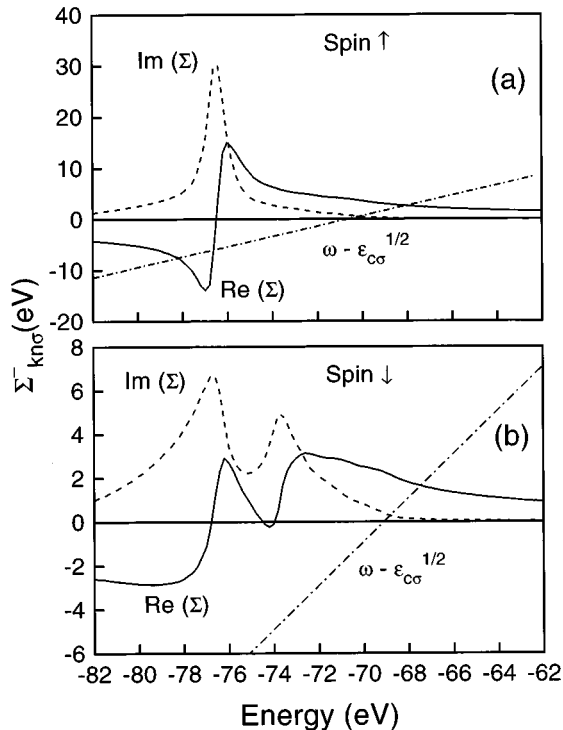


FIG. 8. Self-energy for the creation of majority-spin (a) and minority-spin hole (b) in the core level $3p^{1/2}$.

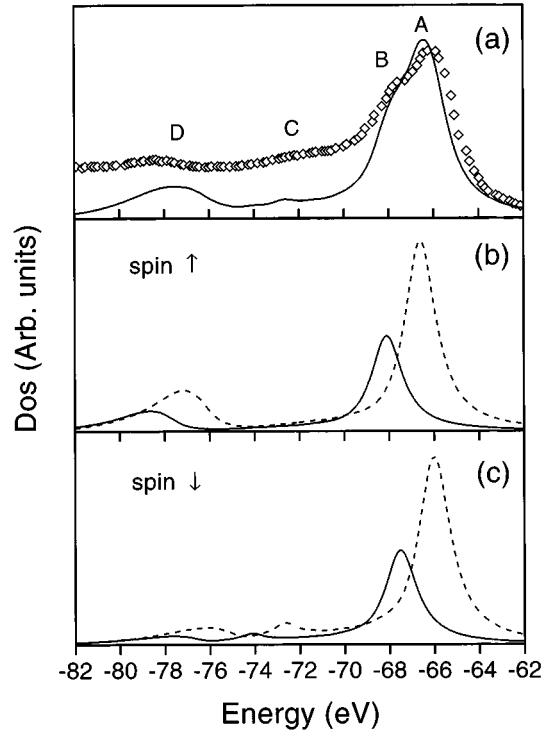


FIG. 9. Spin-integrated spectral function for the creation of a $3p$ core hole compared with the photoemission results of Ref. 3 (a) and its decomposition into contributions from the spin-orbit split level $3p^{1/2}$ (continuous line) and $3p^{3/2}$ (dashed line). (b) refers to majority-spin state and (c) to the minority-spin one.

cess, the strength of the interaction on one side and the number of available states in the valence band on the other. In the case of a minority-spin core hole the weaker parallel spin interaction is compensated by the larger number of empty valence states and both the scattering channels involving parallel and opposite spin particles play a role. The same argument applies to the case of the majority-spin core hole but now the weaker parallel spin interaction is associated to a small number of available empty valence states [see Fig. 2(c)]; for this reason the interaction between opposite spin particles [see Fig. 2(b)] remains the only efficient scattering channel. As a consequence the self-energy for the majority-spin core hole presents a single structure associated to U_{cv} .

As discussed in the preceding section satellite structures are expected to occur at energies where the imaginary part of self-energy has a maximum giving rise to a complex pole of the hole propagator and therefore to a short lived excitation. The structures in the calculated self-energy we have just described and their origin are therefore essential in order to get a physical interpretation of the observed photoemission spectrum. We report in Fig. 9 the calculated spin-integrated spectral density for the creation of a $3p$ core hole compared with the photoemission results of Ref. 22. The spectrum shows a main peak at about 66 eV with two characteristic spin-orbit split structures (A, B) and two satellites (C, D). The decomposition of the spectral function into contributions from the two spin-orbit split levels $3p^{1/2}$ and $3p^{3/2}$ and from different

spins is also shown. The spectral function for the creation of a majority-spin core hole shows a main peak and a satellite for each spin-orbit split level; as discussed above in terms of the self-energy this satellite is associated to the only efficient scattering channel which comes into play after the removal of one majority-spin electron, that is, to configurations of Fig. 2(b) where the majority-spin core hole interacts with opposite spin particles in the valence band, with a strength proportional to U_{cv} . The spectral function for the creation of a minority-spin core hole presents instead two satellites for each spin-orbit split level: the one at the higher binding energy is associated to the configurations of Fig. 2(e) where the spin-down core hole interacts with opposite spin particles in the valence band with a strength proportional to U_{cv} . Due to the small number of empty states available in the spin-up band this satellite is less pronounced here than in the majority-spin spectrum. The satellite at lower binding energy is related to configurations of Fig. 2(f) and to scattering between parallel spin particles of strength proportional to $U_{cv} - J_{cv}$.

The one-to-one correspondence between the configurations of Fig. 2 and the satellite structures allows us to interpret them as shakeup processes occurring after the removal of either a minority- or a majority-spin core electron. The satellite at lower binding energy (C) is then associated to the creation of one minority-spin core hole plus an $e-h$ pair in the valence band of the same spin, giving rise to a bound state of three parallel spin particles which can be defined as a triplet state; the satellite at higher binding energy (D) is related to the creation of either a majority- or a minority-spin core hole plus a valence $e-h$ pair of opposite spin giving rise to a singlet state.

To analyze the spin polarization of the whole core hole spectrum in more detail it is useful to consider the spin-resolved spectra and their difference $D_{\uparrow}^{-}(\omega) - D_{\downarrow}^{-}(\omega)$ reported in Fig. 10. It appears that the spin polarity of structures A, B, C , and D of Fig. 9 is “down,” “up,” “down,” “up,” respectively. This is again in agreement with what has been seen experimentally and reported in Refs. 19, 22, and 23.

VII. SUMMARY

We have described a method for including short-range on-site interactions in the description of both valence and core states of a solid system. When applied to valence states of ferromagnetic nickel the method allows us to get a quasi-particle band structure which compares much more favorably with the experimental observation than conventional mean-field LDA band structure eigenvalues, reproducing the observed bandwidth, the energy dispersion, the satellite structure, and the exchange splitting. Since the method does not rely on a perturbation expansion it has a wide range of application, including any correlation regime. The extension to core levels is quite natural and allows us to take fully into account the itinerant character of valence electrons. We get then a physical picture of the $3p$ core-level spectrum where the spin splitting of the main line is associated to the valence band spin polarization and to the core-valence interaction; the two satellites are interpreted as arising from shakeup processes occurring after the removal of a core elec-

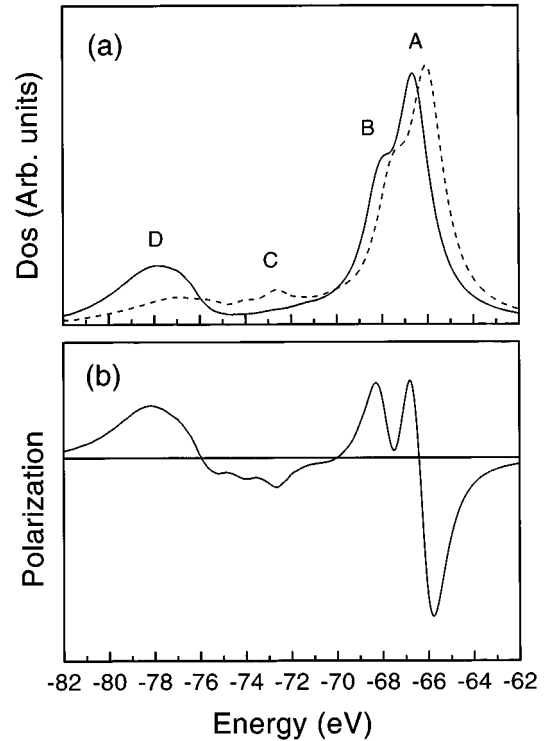


FIG. 10. (a) Calculated spectrum for the creation of a majority-spin (continuous line) and minority-spin (dashed line) $3p$ core hole. (b) Difference spectrum between the two spin components.

tron, involving the creation of a d -band $e-h$ pair. Even though our present choice of empirically determining the parameters of the Hubbard Hamiltonian ensures that we obtain an overall good agreement with experiments we believe that the possibility of reproducing both the satellite structures, the main line, and their spin dependence with just four parameters can be seen as a nontrivial result. The widely used atomic models — which use empirical parameters as well — require also an *ad hoc* evaluation of the so-called extra-atomic effects which allow us to take into account the role of electrons on neighboring atoms;²¹ such effects are on the contrary included here from the beginning since the full details of the valence band structure of the solid system are considered. In this sense the present approach can be considered an appropriate tool to describe the response of an itinerant electron system to the creation of a core hole.

APPENDIX A: MATRIX ELEMENTS OF THE MULTIORBITAL HUBBARD HAMILTONIAN

As discussed in Sec. IV the application of the 3BS method to the valence band states of nickel requires the explicit definition of matrix elements of the Hamiltonian (4.1) containing a noninteracting part that we call here \hat{H}^0 and the on-site interaction among opposite spin electrons that we denote by \hat{H}' . The matrix elements involve states $|s\rangle$ and $|t\rangle$ defined in Eq. (3.5) and pictorially depicted in Fig. 1. We have

$$\begin{aligned}
\langle s|\hat{H}^0|s\rangle &= \sum_{\mathbf{k}'n'\sigma'}^{\text{occ}} \epsilon_{\mathbf{k}'n'\sigma'}^H - \epsilon_{\mathbf{k}n\sigma}^H, \\
\langle s|\hat{H}^0|t\rangle &= 0, \\
\langle t|\hat{H}^0|t\rangle &= \sum_{\mathbf{k}'n'\sigma'}^{\text{occ}} \epsilon_{\mathbf{k}'n'\sigma'}^H + \epsilon_{\mathbf{q}_3n_3-\sigma}^H - \epsilon_{\mathbf{q}_2n_2-\sigma}^H - \epsilon_{\mathbf{q}_1n_1\sigma}^H, \\
\langle s|\hat{H}'|s\rangle &= \sum_{\alpha\beta} \frac{U_{\alpha\beta}}{N} \sum_{\mathbf{k}''n''} |C_{\alpha-\sigma}^{n''}(\mathbf{k}'')|^2 \left\{ \sum_{\mathbf{k}'n'} |C_{\beta\sigma}^{n'}(\mathbf{k}')|^2 - |C_{\beta\sigma}^n(\mathbf{k})|^2 \right\}, \\
\langle s|\hat{H}'|t\rangle &= - \sum_{\alpha\beta} \frac{U_{\alpha\beta}}{N} C_{\alpha-\sigma}^{n_2}(\mathbf{q}_2) * C_{\alpha-\sigma}^{n_3}(\mathbf{q}_3) C_{\beta\sigma}^{n_1}(\mathbf{q}_1) * C_{\beta\sigma}^n(\mathbf{k}) \delta_{\mathbf{k}-\mathbf{q}_1, \mathbf{q}_2-\mathbf{q}_3}, \\
\langle t|\hat{H}'|t\rangle &= \sum_{\alpha\beta} \frac{U_{\alpha\beta}}{N} \left\{ \sum_{\mathbf{k}'n'} |C_{\alpha-\sigma}^{n'}(\mathbf{k}')|^2 \sum_{\mathbf{k}''n''} |C_{\beta\sigma}^{n''}(\mathbf{k}'')|^2 + |C_{\alpha-\sigma}^{n_3}(\mathbf{q}_3)|^2 \sum_{\mathbf{k}'n'} |C_{\beta\sigma}^{n'}(\mathbf{k}')|^2 \right. \\
&\quad \left. - |C_{\alpha-\sigma}^{n_2}(\mathbf{q}_2)|^2 \sum_{\mathbf{k}'n'} |C_{\beta\sigma}^{n'}(\mathbf{k}')|^2 - |C_{\beta\sigma}^{n_1}(\mathbf{q}_1)|^2 \sum_{\mathbf{k}'n'} |C_{\alpha-\sigma}^{n'}(\mathbf{k}')|^2 \right\}, \\
\langle t'|\hat{H}'|t\rangle &= - \sum_{\alpha\beta} \frac{U_{\alpha\beta}}{N} C_{\alpha-\sigma}^{n'_3}(\mathbf{q}'_3) * C_{\alpha-\sigma}^{n_3}(\mathbf{q}_3) C_{\beta\sigma}^{n_1}(\mathbf{q}_1) * C_{\beta\sigma}^{n'_1}(\mathbf{q}'_1) \delta_{\mathbf{q}_2, \mathbf{q}'_2} \delta_{n_2, n'_2} \delta_{\mathbf{q}_1-\mathbf{q}_3, \mathbf{q}'_1-\mathbf{q}'_3} \\
&\quad + \sum_{\alpha\beta} \frac{U_{\alpha\beta}}{N} C_{\alpha-\sigma}^{n_2}(\mathbf{q}_2) * C_{\alpha-\sigma}^{n'_2}(\mathbf{q}'_2) C_{\beta\sigma}^{n_1}(\mathbf{q}_1) * C_{\beta\sigma}^{n'_1}(\mathbf{q}'_1) \delta_{\mathbf{q}_3, \mathbf{q}'_3} \delta_{n_3, n'_3} \delta_{\mathbf{q}_1+\mathbf{q}_2, \mathbf{q}'_1+\mathbf{q}'_2}.
\end{aligned}$$

As discussed in Sec. V the description of core states requires the inclusion of the interaction involving the exchange integral that we call here \hat{H}'' and the extension of the complete set to the three-particle configurations $|z\rangle$ of Fig. 2. It is easy to show that in this case the diagonal matrix elements are similar to the previous ones and that the nonzero off-diagonal ones are $\langle s|\hat{H}'|t\rangle$, $\langle t|\hat{H}'|t'\rangle$, $\langle z|\hat{H}''|z'\rangle$.

APPENDIX B: FADDEEV EQUATIONS FOR THE MULTIBAND HUBBARD HAMILTONIAN

We illustrate the procedure which leads to Eqs. (4.2)–(4.10) for the removal of one spin-up electron. The relationship (3.8) between the diagonal hole propagator and the three-body resolvent is obtained by inserting the completeness relation

$$\sum_s |s\rangle\langle s| + \sum_t |t\rangle\langle t| = 1$$

into the identity

$$\left\langle s \left| (z - \hat{H}^H) \frac{1}{z - \hat{H}^H} \right| s \right\rangle = 1,$$

that is,

$$[z - (H_1)_{ss}]G_{ss}(z) - \sum_t V_{st}G_{ts}(z) = 1. \quad (\text{B1})$$

Since $G_{ts}(z)$ can be obtained by Eq. (3.7) as

$$G_{ts}(z) = \sum_{ts'} F_{tt'} V_{t's'} G_{ss'}(z), \quad (\text{B2})$$

one gets

$$[z - (H_1)_{ss}]G_{ss}(z) - \sum_{tt'} V_{st}V_{t's}F_{tt'}G_{ss} + \sum_{tt'} \sum_{s \neq s'} V_{st}V_{t's'}F_{tt'}G_{ss'} = 1. \quad (\text{B3})$$

By substituting the explicit definition of the matrix elements of \hat{V} it appears that the two summations in Eq. (B3) involve terms of the kind

$$\sum_{\beta\delta} C_{\beta\uparrow}^n(\mathbf{k}) C_{\delta\uparrow}^{n'}(\mathbf{k})^*,$$

with $n = n'$, $n \neq n'$ in the first and second sum, respectively. For this reason it seems reasonable to neglect in Eq. (B3) the last summation with respect to the first one getting in this way Eq. (3.8) as a result.

According to Eq. (3.9) the self-energy is given by the sum

$$\begin{aligned} \sum_{tt'} F_{3tt'} V_{t's} V_{st} &= \frac{U^2}{N^2} \sum_{q_1 q_2 q_3} \sum_{n_1 n_2 n_3} \sum_{\alpha\beta} C_{\alpha\uparrow}^{n_1}(\mathbf{q}_1)^* C_{\alpha\downarrow}^{n_3}(\mathbf{q}_3) C_{\beta\downarrow}^{n_2}(\mathbf{q}_2)^* C_{\beta\uparrow}^n(\mathbf{k}) \\ &\times \sum_{q'_1 q'_2 q'_3} \sum_{n'_1 n'_2 n'_3} \sum_{\gamma\delta} C_{\gamma\uparrow}^{n'_1}(\mathbf{q}'_1) C_{\gamma\downarrow}^{n'_3}(\mathbf{q}'_3)^* C_{\delta\downarrow}^{n'_2}(\mathbf{q}'_2) C_{\delta\uparrow}^n(\mathbf{k})^* \langle \mathbf{q}_1 n_1 \uparrow \mathbf{q}_2 n_2 \downarrow \mathbf{q}_3 n_3 \downarrow | | \hat{F}_3^D \\ &+ \hat{F}_3^D (\hat{S}_{h-e} + \hat{T}_{h-h} \hat{F}_3^D \hat{S}_{h-e}) \hat{F}_3^D | \mathbf{q}'_1 n'_1 \uparrow \mathbf{q}'_2 n'_2 \downarrow \mathbf{q}'_3 n'_3 \downarrow \rangle, \end{aligned} \quad (\text{B4})$$

where we have used the definition (3.5) for $|t\rangle$ and $|t'\rangle$. Let us define now the orbital-dependent free propagator describing h - h scattering,

$$g_3^{\alpha\beta}(\mathbf{q}_3 n_3 \omega) = \frac{1}{N^2} \sum_{q_1 n_1 q_2 n_2} \frac{C_{\alpha\uparrow}^{n_1}(\mathbf{q}_1)^* C_{\alpha\downarrow}^{n_1}(\mathbf{q}_1) C_{\beta\downarrow}^{n_2}(\mathbf{q}_2)^* C_{\beta\uparrow}^{n_2}(\mathbf{q}_2)}{\omega - (E_0 - \epsilon_{\mathbf{q}_1 n_1 \uparrow}^{\text{MF}} - \epsilon_{\mathbf{q}_2 n_2 \downarrow}^{\text{MF}} + \epsilon_{\mathbf{q}_3 n_3 \downarrow}^{\text{MF}})},$$

where the summation is over filled states of band indices n_1 and n_2 . By using the definition (3.11) it is easy to show that

$$\sum_{q_1 n_1 q_2 n_2} C_{\alpha\uparrow}^{n_1}(\mathbf{q}_1)^* C_{\beta\downarrow}^{n_2}(\mathbf{q}_2)^* \langle \mathbf{q}_1 n_1 \uparrow \mathbf{q}_2 n_2 \downarrow \mathbf{q}_3 n_3 \downarrow | \hat{G}_3^D \hat{T}_{h-h} | \mathbf{q}'_1 n'_1 \uparrow \mathbf{q}'_2 n'_2 \downarrow \mathbf{q}'_3 n'_3 \downarrow \rangle = \frac{C_{\alpha\uparrow}^{n_1}(\mathbf{q}_1)^* C_{\beta\downarrow}^{n_2}(\mathbf{q}_2)^* g_3^{\alpha\beta}(\mathbf{q}_3 \omega)}{1 - U_{\alpha\beta} g_3^{\alpha\beta}(\mathbf{q}_3 \omega)} \delta_{\mathbf{q}_3, \mathbf{q}'_3}.$$

It is also useful to define the orbital-dependent t matrix for h - h scattering,

$$T_{h-h}^{\alpha\beta}(\mathbf{q}_3 n_3 \omega) = \frac{U_{\alpha\beta}}{1 - U_{\alpha\beta} g_3^{\alpha\beta}(\mathbf{q}_3 n_3 \omega)}.$$

Similar definitions and relations hold for e - h scattering. It is then a matter of simple algebra to transform Eq. (B4) into the form

$$\sum_{tt'} F_{3tt'} V_{t's} V_{st} = \sum_{\beta} |C_{\beta}^n(\mathbf{k}\uparrow)|^2 - \sum_{\alpha} \frac{U_{\alpha\beta}}{N} \sum_{\mathbf{q}_3 n_3} \{ |C_{\beta}^n(\mathbf{q}_3 \downarrow)|^2 + T_{h-h}^{\alpha\beta}(\mathbf{q}_3 n_3) [|C_{\beta}^n(\mathbf{q}_3 \downarrow)|^2 + U_{\alpha\beta} A^{\alpha\beta}(\mathbf{q}_3 n_3)] \},$$

where

$$\begin{aligned} A^{\alpha\beta}(\mathbf{q}_3 n_3) &= \frac{1}{N} \sum_{q_1 q_2} \sum_{n_1 n_2} C_{\alpha\uparrow}^{n_1}(\mathbf{q}_1)^* C_{\beta\downarrow}^{n_2}(\mathbf{q}_2)^* C_{\alpha\downarrow}^{n_3}(\mathbf{q}_3) \sum_{q'_1 q'_2 q'_3} \sum_{n'_1 n'_2 n'_3} C_{\gamma\uparrow}^{n'_1}(\mathbf{q}'_1) C_{\gamma\downarrow}^{n'_3}(\mathbf{q}'_3)^* C_{\delta\downarrow}^{n'_2}(\mathbf{q}'_2) \\ &\times \langle \mathbf{q}_1 n_1 \uparrow \mathbf{q}_2 n_2 \downarrow \mathbf{q}_3 n_3 \downarrow | \hat{F}_3^D \hat{S}_{h-e} \hat{F}_3^D | \mathbf{q}'_1 n'_1 \uparrow \mathbf{q}'_2 n'_2 \downarrow \mathbf{q}'_3 n'_3 \downarrow \rangle. \end{aligned}$$

From now on the procedure is the same as the one described in Ref. 6, adopting in particular the so-called local approximation¹⁰ which allows us to transform all the summations over k vectors into integrals involving the density of states.

¹L. C. Davis, J. Appl. Phys. **59**, R25 (1986), and references therein.

²Y. Kakehashi, K. Becker, and P. Fulde, Phys. Rev. B **29**, 16 (1984).

³A. K. See and L. E. Klebanoff, Phys. Rev. B **51**, 11 002 (1995).

⁴F. Manghi, C. Calandra, and S. Ossicini, Phys. Rev. Lett. **73**,

3129 (1994).

⁵J. Igarashi, J. Phys. Soc. Jpn. **52**, 2827 (1983).

⁶C. Calandra and F. Manghi, Phys. Rev. B **50**, 2061 (1994).

⁷A. Villaforita, F. Manghi, F. Parmigiani, and C. Calandra (unpublished).

⁸J. Igarashi, J. Phys. Soc. Jpn. **54**, 260 (1985).

⁹F. Aryasetiawan, Phys. Rev. B **46**, 13 051 (1992).

- ¹⁰G. Treglia, F. Ducastelle, and D. Spanjaard, *J. Phys. (France)* **41**, 281 (1980); **43**, 341 (1982).
- ¹¹L. Kleinman and K. Mednick, *Phys. Rev. B* **24**, 6880 (1982).
- ¹²R. G. Jordan and M. A. Hoyland, *Solid State Commun.* **72**, 433 (1989).
- ¹³M. M. Steiner, R. C. Albers, and L. J. Sham, *Phys. Rev. B* **45**, 13 272 (1992).
- ¹⁴A. Liebsch, *Phys. Rev. Lett.* **43**, 1431 (1979).
- ¹⁵C. Calandra and F. Manghi, *Phys. Rev. B* **45**, 5819 (1992).
- ¹⁶Jun-ichi Igarashi, P. Unger, K. Hirai, and P. Fulde, *Phys. Rev. B* **49**, 16 181 (1994).
- ¹⁷C. S. Fadley and D. Shirley, *Phys. Rev. A* **2**, 1109 (1970).
- ¹⁸C. Carbone, T. Kachel, R. Rochow, and W. Gudat, *Solid State Commun.* **77**, 619 (1991).
- ¹⁹T. Kachel, C. Carbone, and W. Gudat, *Phys. Rev. B* **47**, 15 391 (1993); C. Carbone, T. Kachel, R. Rochow, and W. Gudat, *Z. Phys. B* **79**, 325 (1990).
- ²⁰B. T. Thole and G. van der Laan, *Phys. Rev. B* **44**, 12 424 (1991).
- ²¹A. K. See and L. E. Klebanoff, *Phys. Rev. Lett.* **74**, 1454 (1995).
- ²²Y. Liu, Z. Xu, Pd. Johnson, and G. van der Laan, *Phys. Rev. B* **52**, R8593 (1995).
- ²³Y. Saitoh, T. Matsushita, S. Imada, H. Daimon, S. Suga, J. Fujii, and K. Shimada *et al.* *Phys. Rev. B* **52**, R11549 (1995).
- ²⁴L. D. Faddeev, *Zh. Eksp. Teor. Fiz.* **39**, 1459 (1960) [*Sov. Phys. JETP* **12**, 1014 (1961)].
- ²⁵P. H. Dederichs, S. Blugel, R. Zeller, and H. Akai, *Phys. Rev. Lett.* **53**, 2512 (1984).
- ²⁶O. K. Andersen, *Phys. Rev. B* **12**, 3060 (1975).
- ²⁷O. K. Andersen and O. Jepsen, *Phys. Rev. Lett.* **53**, 2571 (1984).
- ²⁸T. J. Kreutz, P. Aebi, and J. Osterwalder, *Solid State Commun.* **96**, 339 (1995).
- ²⁹Y. Sakisaka, T. Komeda, M. Onchi, H. Kato, S. Masuda, and K. Yagi, *Phys. Rev. B* **36**, 6383 (1987).